Scanning tunneling microscopy detection of spin polarized resonant surface bands: The example of Fe(001)

Athanasios N. Chantis,[1,*] Darryl L. Smith,[1] J. Fransson,[2] and A. V. Balatsky[1,3]
[1]*Theoretical Division, Los Alamos National Laboratory, Los Alamos, New Mexico 87545, USA*
[2]*Department of Physics and Materials Science, Uppsala University, P.O. Box 530, SE-751 21 Uppsala, Sweden*
[3]*Center for Integrated Nanotechnology, Los Alamos National Laboratory, Los Alamos, New Mexico 87545, USA*
(Received 19 September 2008; revised manuscript received 6 February 2009; published 17 April 2009)

We study theoretically the effect of a spin polarized resonant surface band on the conductance of scanning tunneling spectroscope with a spin polarized tip (SP-STM). Using the example of the Fe(001) surface, we show that a minority-spin surface state can induce a bias dependence of the tunneling differential conductance which depends strongly on the orientation of the magnetization in the SP-STM tip relative to the magnetization axis in the surface. We propose the use of this effect to determine the spin character of the surface band.

DOI: 10.1103/PhysRevB.79.165423 PACS number(s): 73.23.−b, 72.25.Mk, 73.40.Gk, 73.40.Rw

I. INTRODUCTION

The properties of magnetic surfaces and interfaces have attracted recently a lot of attention because of the advent of spintronics, a technology aiming to harness electron's spin in data storage and processing, typically utilizing heterostructures composed of magnetic and nonmagnetic materials.[1] It is well known that many transition-metal surfaces, as well as their interfaces with insulators, exhibit electronic bands that are localized at the surface or interface. If such a band does not mix with bulk states, it is called a localized surface band. If it mixes weakly with bulk bands, it broadens and becomes a resonant surface band. Resonant surface or interface bands can contribute strongly to the tunneling current[2–10] and influence the spin polarization of the tunneling electrons.[9] Therefore, it is important to understand the spin character of such states. Scanning tunneling microscopy (STM) is a well-established technique for imaging surface structures[11–14] and for spectroscopic measurements of local structures and inhomogeneities on surfaces.[15–17] Recent developments of STM tools with a spin polarized tip (SP-STM) allow for controllable measurements of magnetic[18–20] and spin-dynamical[21] features and local magnetic structures.[22] Spin polarized tunneling for STM has been theoretically studied with respect to noise[23] and spin detection and spin reversal of local spins located on a substrate surface.[24,25]

Here, we propose the use of SP-STM for detection of spin polarized surface resonant bands and the determination of their spin character. Unlike photoemission, SP-STM can probe both the occupied and unoccupied states of a *clean* surface in a wide energy range above and below the Fermi energy. This is particularly useful because a spin polarized surface band in the unoccupied part of the spectrum is important for spin polarized electron *extraction* at a surface (interface) in the same way that a spin polarized surface band in the occupied part of the spectrum is important for electron *injection*. Also, it is difficult to know from photoemission experiments alone how strongly an observed surface state contributes to the spin polarized tunneling current. A strongly localized spin polarized surface band can have weak contribution to the tunneling current and therefore does not influence the spin polarization of the total current in a decisive way.

It is important to understand the effect of a spin polarized surface band on the SP-STM conductance. The surface band structure can be complicated,[8] therefore the magnetic structure inferred from SP-STM has to be interpreted carefully. In this paper, we show how the surface band structure can bring additional complexity in the energy and momentum dependence of tunneling matrix elements and affect the interpretation of SP-STM data. As a case study, we consider the Fe(001) surface. The electronic and magnetic structures of the Fe(001) surface have been studied in great detail theoretically using first-principles methods.[8,26–28] These calculations show the presence of a *minority*-spin polarized surface band in the vicinity of Fermi level. Using STM, Stroscio *et al.*[29] provided solid experimental evidence that such a surface band exists and can have a significant contribution to the tunneling current. However, this experiment was incapable of distinguishing the *spin character* of the surface resonant band. To date, the spin- and angular-resolved photoemission (SARPES) evidence on the spin character of this surface band is controversial.[30–33] For example, Brookes *et al.*[30] identified a *minority* surface resonance at $\bar{\Gamma}$ and a minority surface state at $\bar{X}$ in the surface Brillouin zone, while Sawada *et al.*[31] concluded that the observed occupied surface states belong to a *majority*-spin surface band located just below the Fermi energy along the $\bar{\Gamma}$-$\bar{\Delta}$-$\bar{X}$ symmetry line. We are not aware of any *direct* observation of the spin character of unoccupied surface states of a clean Fe(001) surface.

Here, we consider an ideal SP-STM tip and a planar Fe surface, within the linear-response approximation. Previous linear-response studies[34] based only on the surface density of states were able to give a satisfactory explanation of the SP-STM conductance. Our approach, in addition to the *ab initio* surface density of states, incorporates the energy and momentum dependence of the tunneling matrix elements. Since we are interested in determining the influence of the surface resonant bands of the sample on the spin-dependent STM tunneling current, we consider a case in which the tunneling matrix elements do not depend strongly on the electronic structure and geometry of the STM tip. It is important to design the SP-STM tip so that the experimental results depend strongly on the electronic structure of the sample and weakly on the electronic structure of the SP-STM tip.

We find that a complex angle and energy dependence of the tunneling differential conductance emerge as a result of the energy and momentum dependence of minority-spin band structure in Fe(001) surface. Our results identify a specific route to determine the spin character of the Fe(001) surface band with the help of SP-STM. The proposed experiment can probe both occupied and unoccupied surface states depending on whether the tunneling current is from or into the surface, respectively. These results are applicable to a broad set of materials where the minority- or majority-spin structure exhibits nontrivial energy dependence.

The rest of this article is organized as follows. In Sec. II we discuss our numerical approach and present our results. Particular emphasis is given to the relation of our approach to the Tersoff and Hamann formula for the tunneling current in STM.[35] Then, based on the obtained results we discuss our proposal on how to detect the spin character of surface states with the help of SP-STM. Section III presents our conclusions.

II. APPROACH AND RESULTS

We first consider an Fe/vacuum/Cu tunnel structure with a nonmagnetic bcc Cu electrode. The bcc Cu electrode has a spin-independent free-electron-like band structure and a featureless surface transmission function.[3] As a result, it does not strongly influence the transverse wave vector dependence of the tunneling matrix elements. Therefore this electrode simulates an ideal STM tip in which the tunneling current depends strongly on the electronic properties of the sample and weakly on the electronic properties of the probe. Calculations are performed for the majority- and minority-spin components of the Fe sample separately. To simulate spin polarization in the STM tip, we weigh the two spin components of the calculated tunneling current with a spin polarization factor. The structure considered consists of a semi-infinite Fe region, several layers of vacuum (empty atomic spheres), and a semi-infinite Cu region. This approach avoids possible artifacts due to interference between surface resonances at the two metallic electrodes.[10] When two resonant states occur on opposite contacts and are located in the same $(E,\mathbf{k}_{\|})$ space, resonant transmission can occur across the structure. In real structures such resonances are unlikely because the symmetry of the structure is broken by geometry and applied bias.

The calculational approach is based on the Green's function representation of the tight-binding linear muffin-tin orbital (TB-LMTO) method in the atomic sphere approximation (ASA).[36] We use third-order parametrization for the Green's function.[37] The electronic structure problem is solved within the scalar relativistic density functional theory (DFT) where the exchange and correlation potentials are treated in the local spin density approximation (LSDA). The conductance is calculated with the principal-layer Green's function technique[38–40] within the Landauer-Büttiker approach.[41] The semi-infinite Fe and Cu electrodes are separated by approximately 1 nm of vacuum represented by six monolayers of empty atomic spheres. The structure is oriented in the [001] direction. Self-consistent charge distribution is achieved before the transport calculations are performed. The spin-dependent $\mathbf{k}_{\|}$-integrated transmission

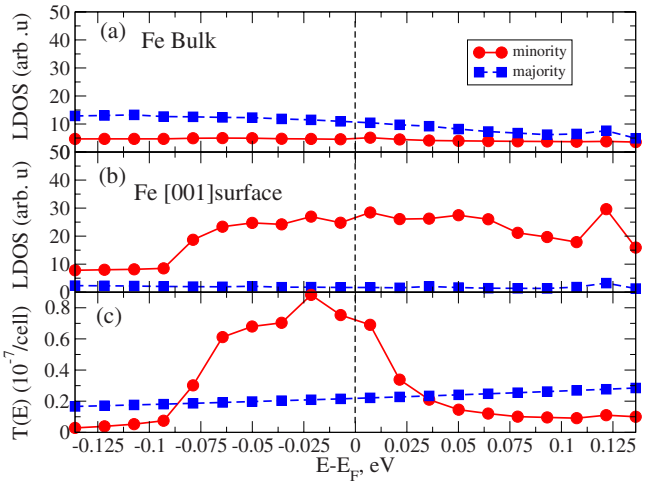

FIG. 1. (Color online) (a) Spin-resolved DOS for the bulk Fe. (b) Spin-resolved DOS for the Fe(001) surface. (c) Spin-resolved $\mathbf{k}_{\|}$-integrated transmission for the Fe/vaccum/Cu as a function of energy. The Fermi level is at zero energy.

$$T^{\sigma}(E) = 1/2\pi \int_{2\mathrm{DBZ}} t^{\sigma}(E,\mathbf{k}_{\|}) d^2\mathbf{k}_{\|} \tag{1}$$

is calculated in the window from E_F to E_F+eV. Here, $t^{\sigma}(E,\mathbf{k}_{\|})$ is the transmission coefficient and $\sigma=\uparrow,\downarrow$ ($\uparrow$ =majority spin, $\downarrow$=minority spin). The spin-quantization axis lies along (001) direction. A uniform 250×250 mesh was used for the integration in the two-dimensional Brillouin zone (2DBZ). With this transmission we determine the current density

$$J^{\sigma}(V) = e/h \int_{E_F}^{E_F+\mathrm{eV}} T^{\sigma}(E) dE. \tag{2}$$

This is an excellent approximation appropriate for comparison to experiment when the applied voltages are small. The spin-resolved differential conductance is $dJ^{\sigma}/dV \propto T(E_F+\mathrm{eV})$.

Figures 1(a) and 1(b) show the calculated Fe bulk spin-resolved density of states (DOS) and local DOS (LDOS) of the Fe monolayer at the Fe(001) surface, respectively. The energies are given with respect to the Fermi level E_F. In the Fe bulk [Fig. 1(a)] the majority spin dominates over the minority spin throughout the entire energy interval shown here. However, in the surface monolayer [Fig. 1(b)] the spin polarization of the DOS is totally reversed; it is the minority spin that dominates over the majority spin throughout the entire energy interval. In Refs. 8 and 9 it was shown that this reversal is caused by Fe 3*d* surface states of minority spin. As shown in Fig. 1(c), sign reversal of the spin polarization of the surface DOS does not necessarily lead to sign reversal of the spin polarization of tunneling transmission, at least throughout the same energy interval.

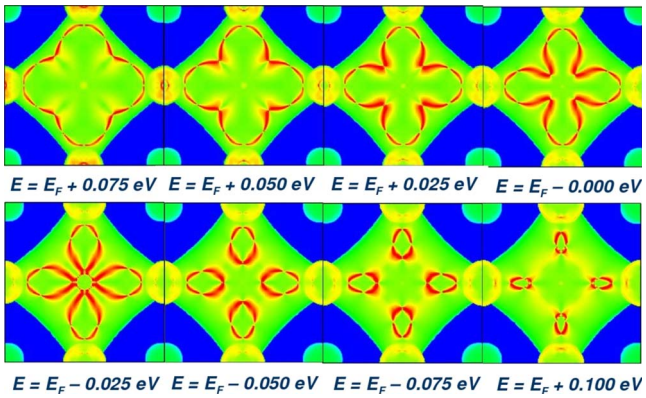

FIG. 2. (Color online) Minority-spin $\mathbf{k}_\parallel$-resolved DOS of the Fe(001) surface for different energies around the Fermi level. The abscissa is along [100] and the ordinate is along [010]. The maximum value is represented by red (light gray), the minimum by blue (dark gray).

In Fig. 2 we present the minority-spin $\mathbf{k}_\parallel$-resolved DOS of the Fe(001) surface for different energies around the Fermi level. The bright red (light gray) features on these plots are created by the surface band. The surface band has C_{4v} symmetry which is the symmetry of the Fe(001) surface. These bands are dominated by the minority-spin surface states arising from $d_{x^2-y^2}$ and d_{xy} orbitals on surface Fe sites that couple with the bulk Fe $\Delta_{2'}$ minority band. Unlike the majority-spin bulk band this band never crosses the 2DBZ at the Γ point. The closest it gets to the Γ point is at the energy of $E_F-0.025$ eV where we see a bright four-petal structure centered at the Γ point without touching it. Considering that $\mathbf{k}_\parallel$ is conserved during tunneling across an ideal surface, for an electron deep in the vacuum region the leading order decay rate of the electron wave function is proportional to $\exp[-(\kappa^2+\mathbf{k}_\parallel^2)^{1/2}z]$, where κ is the decay rate for normal incidence which is determined by the work function. The tunneling transmission for a given energy is also proportional to the total number of states at this energy $n_\sigma(E)$. In Fig. 1(c) one can compare the spin-resolved tunneling transmission to the spin-resolved surface DOS. We see the influence of both factors mentioned above in the polarization of the transmission coefficient. The minority-spin transmission dominates over the majority spin for a large part of the energy interval due to its higher surface DOS. For the energy $E=E_F-0.025$ eV, the minority-spin transmission has a maximum and in the energy interval where the minority-spin DOS is flat, the minority-spin transmission is less when the surface states are further away from the Γ point. For energies where the minority-spin surface states are far away from the center of the 2DBZ, the minority-spin transmission is less than the majority spin even though for the same energy the minority-spin surface DOS is much larger than the majority spin. For larger distances between the Cu counterelectrode and the Fe surface the ratio of minority-spin transmission to majority-spin transmission should become even less for all energies in the shown interval. Our calculations show that for a distance twice as big, the change of spin polarization bias dependence is not very large while the current drops by about 4 orders of magnitude. This shows that within the range of distances available to an SP-STM tip, the inversion of spin polarization should be detectable. In our calculations, the minority-spin peak of the transmission is located slightly below the Fermi energy. This is in agreement with previous ASA calculations of the Fe(001) LDOS in the vacuum region.[27] Because of the simple Cu tip that we are using to calculate the transmission, this agreement is expected. However, we also note that as it was shown in Ref. 27 ASA may result in a small error of the LDOS peak in the vacuum region due to its spherical approximation of the potential. This does not affect the following discussion qualitatively.

We relate our results from the planar calculation to the STM experiment. Following Tersoff and Hamann,[35] the STM tunneling current at 0 K is given by

$$I^\sigma(V) \propto \sum_{\mathbf{pk}} f[E_i^\sigma(\mathbf{p})+\mathrm{eV}]\{1-f[E_j^\sigma(\mathbf{k})]\} \times |\langle i,\mathbf{p}|T^\sigma|j,\mathbf{k}\rangle|^2 \delta[E_i^\sigma(\mathbf{p})-E_j^\sigma(\mathbf{k})], \quad (3)$$

where f is the Fermi function and $|\langle i,\mathbf{p}|T^\sigma|j,\mathbf{k}\rangle|$ is the tunneling matrix element between initial and final tunneling states. Here, we designate the electron state labels by $\mathbf{p}(\mathbf{k})$ and let $i(j)$ denote the STM tip (Fe sample). We specially consider the case that electrons tunnel from the STM tip to the Fe sample for positive voltage V. An analogous argument applies for tunneling in the other direction. Because of the energy-conserving δ function, we have can set $E_i^\sigma(\mathbf{p})$ equal to $E_j^\sigma(\mathbf{k})$ and take the sum on $\mathbf{p}$ across the Fermi functions

$$I^\sigma(V) \propto \sum_{\mathbf{k}} f[E_j^\sigma(\mathbf{k})+\mathrm{eV}]\{1-f[E_j^\sigma(\mathbf{k})]\} \times \sum_{\mathbf{p}} |\langle i,\mathbf{p}|T^\sigma|j,\mathbf{k}\rangle|^2 \delta[E_i^\sigma(\mathbf{p})-E_j^\sigma(\mathbf{k})]. \quad (4)$$

For the an ideal STM tip, the tunneling matrix element does not depend strongly on the electron state in the tip $\mathbf{p}$ and we can take the squared matrix element across the sum on states in the tip giving

$$I^\sigma(V) \propto \sum_{\mathbf{k}} f[E_j^\sigma(\mathbf{k})+\mathrm{eV}]\{1-f[E_j^\sigma(\mathbf{k})]\} \times |\langle i|T^\sigma|j,\mathbf{k}\rangle|^2 D_i^\sigma[E_j^\sigma(\mathbf{k})], \quad (5)$$

where $D_i^\sigma[E_j^\sigma(\mathbf{k})]$ is the density of states for spin σ in the tip. Equation (3) has the same form as Eq. (2) except for the spin-dependent density of states in the tip $D_i^\sigma[E_j^\sigma(\mathbf{k})]$. For an ideal SP-STM tip we take this density of states to depend on degree and direction of spin polarization in the tip, but to be slowly varying with energy. Then $D_i^\sigma(E_j^\sigma(\mathbf{k}))\rightarrow(1+P)$ for the majority-spin polarization direction in the SP-STM tip and $D_i^\sigma(E_j^\sigma(\mathbf{k}))\rightarrow(1-P)$ for the majority-spin polarization direction in the SP-STM tip, where P is the degree of spin polarization of the SP-STM tip.

Based on these results, we discuss the possibility of detecting the spin character of Fe surface states with a ferromagnetic (FM) tip. Let us assume that the spin-quantization axis in the FM tip is rotated by an angle θ relatively to the

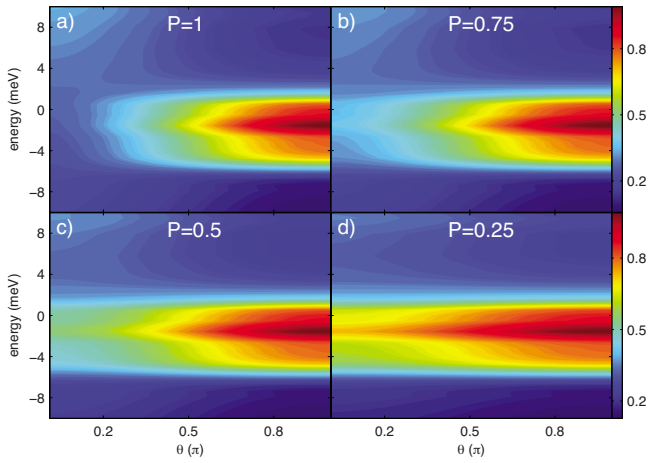

FIG. 3. (Color online) The energy dependence of the differential conductance of a FM tip as we rotate the direction of the magnetization in the tip by an angle θ relatively to the magnetization in Fe. We show four different cases of DOS spin polarization P of the tip. The bright red (light gray) regions observed for $\theta=\pi$ are created by the minority-spin transmission peaks in Fig. 1(c).

spin-quantization axis in the Fe surface. The spin components of the electron wave function in the tip can be written as

$$|\uparrow,\theta\rangle = \cos(\theta/2)|\uparrow\rangle - i\,\sin(\theta/2)|\downarrow\rangle,$$

$$|\downarrow,\theta\rangle = -i\,\sin(\theta/2)|\uparrow\rangle + \cos(\theta/2)|\downarrow\rangle, \tag{6}$$

where $|\sigma,\theta\rangle$ ($\sigma=\uparrow,\downarrow$) are the spin states in the SP-STM tip and $|\sigma\rangle$ are the spin states in the Fe sample. The total transmission coefficient for an arbitrary spin polarization P of the tip can be written as

$$\begin{aligned} T &= (1+P)T^{\uparrow}\cos^2(\theta/2) + (1-P)T^{\uparrow}\sin^2(\theta/2) \\ &\quad + (1+P)T^{\downarrow}\sin^2(\theta/2) + (1-P)T^{\downarrow}\cos^2(\theta/2) \\ &= (T^{\uparrow}+T^{\downarrow}) + (T^{\uparrow}-T^{\downarrow})P\cos\,\theta, \end{aligned} \tag{7}$$

where $T^{\uparrow,\downarrow}$ are the spin components of the transmission coefficient (differential conductance) presented in Fig. 1(c). When $\theta=0$ the spin-quantization axis in the tip is parallel to majority spins in Fe and when $\theta=180$ it is parallel to minority spin.

In Fig. 3 we show the energy dependence of the differential conductance of a FM tip as we rotate the direction of the magnetization in the tip by an angle θ relatively to the magnetization in the Fe. Four different cases of DOS spin polarization P of the tip are shown. In the general case, $0<P<1$, a complicated energy-angular dependence is observed. However, the trends can be easily understood from the two limiting cases of $P=1$ (half-metallic tip) and $P=0$ (not shown in Fig. 3 but can be extrapolated from the case of $P=0.25$). For $P=1$ the energy dependence of the transmission for $\theta=0$ is identical to the majority-spin transmission in Fig. 1(c), while for $\theta=180$ the energy dependence is identical to that of minority spin in Fig. 1(c) [to facilitate the comparison in Fig. 4 we provide a three-dimensional version of Fig. 3(a)]. As we decrease the degree of spin polarization in the tip the angular dependence of the differential conductance becomes less pronounced. As it should be, at the limit of $P=0$ the differential conductance becomes independent of the angle and equal to the sum $T^{\uparrow}+T^{\downarrow}$. This case corresponds to the conventional (nonmagnetic tip) STM measurement by Stroscio *et al.*[29]

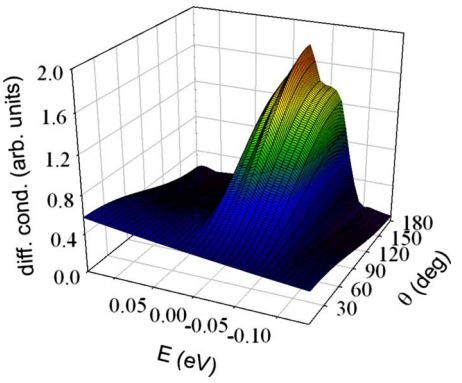

FIG. 4. (Color online) A three-dimensional plot of differential conductance as a function of energy and relative direction of spin orientation in the sample and tip for $P=1$

III. CONCLUSION

In conclusion we have shown that unlike a conventional STM which only can measure a sharp peak in the energy dependence of the differential conductance when a localized surface band is present, a SP-STM measurement should be able to measure an angular dependence as well. In the general case of $0<P<1$ a complicated energy-angular dependence emerges but the trends can be easily understood from the limit of a half-metallic, $P=1$, tip. The energy dependence of the differential conductance in this case will be monotonic for either parallel or antiparallel direction of the magnetization of the STP tip relative to the direction of the easy axis in the Fe(001) surface. This can be used to extract the spin character of the surface band.

ACKNOWLEDGMENTS

The work at Los Alamos National Laboratory was supported by DOE Office of Basic Energy Sciences Work Proposal No. 08SCPE973.

*achantis@lanl.gov

[1] I. Zutic, J. Fabian, and S. D. Sarma, Rev. Mod. Phys. **76**, 323 (2004).

[2] O. Wunnicke, N. Papanikolaou, R. Zeller, P. H. Dederichs, V. Drchal, and J. Kudrnovský, Phys. Rev. B **65**, 064425 (2002).

[3] K. D. Belashchenko, E. Y. Tsymbal, M. van Schilfgaarde, D. A. Stewart, I. I. Oleinik, and S. S. Jaswal, Phys. Rev. B **69**, 174408 (2004).

[4] K. D. Belashchenko, E. Y. Tsymbal, I. I. Oleynik, and M. van Schilfgaarde, Phys. Rev. B **71**, 224422 (2005).

[5] K. D. Belashchenko, J. Velev, and E. Y. Tsymbal, Phys. Rev. B **72**, 140404(R) (2005).

[6] J. P. Velev, K. D. Belashchenko, and E. Y. Tsymbal, Phys. Rev. Lett. **96**, 119601 (2006).

[7] K. Palotás and W. A. Hofer, J. Phys.: Condens. Matter **17**, 2705 (2005).

[8] A. N. Chantis, K. D. Belashchenko, E. Y. Tsymbal, and M. van Schilfgaarde, Phys. Rev. Lett. **98**, 046601 (2007).

[9] A. N. Chantis, K. D. Belashchenko, D. L. Smith, E. Y. Tsymbal, M. van Schilfgaarde, and R. C. Albers, Phys. Rev. Lett. **99**, 196603 (2007).

[10] M. N. Khan, J. Henk, and P. Bruno, J. Phys.: Condens. Matter **20**, 155208 (2008).

[11] G. Binnig, H. Rohrer, C. Gerber, and E. Weibel, Appl. Phys. Lett. **40**, 178 (1982).

[12] G. Binnig, H. Rohrer, C. Gerber, and E. Weibel, Phys. Rev. Lett. **49**, 57 (1982).

[13] G. Binnig, H. Rohrer, C. Gerber, and E. Weibel, Phys. Rev. Lett. **50**, 120 (1983).

[14] G. Binnig, H. Rohrer, C. Gerber, and E. Weibel, Surf. Sci. **131**, L379 (1983).

[15] M. F. Crommie, C. P. Lutz, and D. M. Eigler, Nature (London) **363**, 524 (1993).

[16] C. F. Hirjibehedin, C. P. Lutz, and A. J. Heinrich, Science **312**, 1021 (2006).

[17] C. F. Hirjibehedin, C.-Y. Lin, A. F. Otte, M. Ternes, C. P. Lutz, B. A. Jones, and A. J. Heinrich, Science **317**, 1199 (2007).

[18] S. Heinze, M. Bode, A. Kubetzka, O. Pietzsch, X. Nie, S. Blügel, and R. Wiesendanger, Science **288**, 1805 (2000).

[19] A. Wachowiak, J. Wiebe, M. Bode, O. Pietzsch, M. Morgenstern, and R. Wiesendanger, Science **298**, 577 (2002).

[20] M. Bode, M. Heide, K. von Bergmenn, P. Ferriani, S. Heinze, G. Bihlmayer, A. Kubetzka, O. Pietzsch, S. Blügel, and R. Wiesendanger, Nature (London) **447**, 190 (2007).

[21] F. Meier, L. Zhou, J. Wiebe, and R. Wiesendanger, Science **320**, 82 (2008).

[22] P. Gambardella, S. Rusponi, M. Veronese, S. S. Dhesi, C. Grazioli, A. Dallmeyer, I. Cabria, R. Zeller, P. H. Dederichs, K. Kern *et al.*, Science **300**, 1130 (2003).

[23] Z. Nussinov, M. F. Crommie, and A. V. Balatsky, Phys. Rev. B **68**, 085402 (2003).

[24] J. Fransson, Phys. Rev. B **77**, 205316 (2008).

[25] J. Fransson, Nanotechnology **19**, 285714 (2008).

[26] S. Ohnishi, A. J. Freeman, and M. Weinert, Phys. Rev. B **28**, 6741 (1983).

[27] N. Papanikolaou, B. Nonas, S. Heinze, R. Zeller, and P. H. Dederichs, Phys. Rev. B **62**, 11118 (2000).

[28] T. Asada, G. Bihlmayer, S. Handschuh, S. Heinze, P. Kurz, and S. Blugel, J. Phys.: Condens. Matter **11**, 9347 (1999).

[29] J. A. Stroscio, D. T. Pierce, A. Davies, R. J. Celotta, and M. Weinert, Phys. Rev. Lett. **75**, 2960 (1995).

[30] N. B. Brookes, A. Clarke, P. D. Johnson, and M. Weinert, Phys. Rev. B **41**, 2643 (1990).

[31] M. Sawada, A. Kimura, and A. Kakizaki, Solid State Commun. **109**, 129 (1998).

[32] P. D. Johnson, Y. Chang, N. B. Brookes, and M. Weinert, J. Phys.: Condens. Matter **10**, 95 (1998).

[33] E. Vescovo, O. Rader, and C. Carbone, Phys. Rev. B **47**, 13051 (1993).

[34] M. Bode, S. Heinze, A. Kubetzka, O. Pietzsch, X. Nie, G. Bihlmayer, S. Blügel, and R. Wiesendanger, Phys. Rev. Lett. **89**, 237205 (2002).

[35] J. Tersoff and D. R. Hamann, Phys. Rev. B **31**, 805 (1985).

[36] O. K. Andersen, Phys. Rev. B **12**, 3060 (1975).

[37] O. Gunnarsson, O. Jepsen, and O. K. Andersen, Phys. Rev. B **27**, 7144 (1983).

[38] I. Turek, V. Drchal, J. Kudrnovský, M. Šob, and P. Weinberger, *Electronic Structure of Disordered Alloys, Surfaces and Interfaces* (Kluwer, Dordrecht, 1997).

[39] J. Kudrnovský, V. Drchal, C. Blaas, P. Weinberger, I. Turek, and P. Bruno, Phys. Rev. B **62**, 15084 (2000).

[40] A. N. Chantis, T. Sandu, and J. L. Xu, PMC Phys. B **1**, 13 (2008).

[41] S. Datta, *Electronic Transport in Mesoscopic Systems* (Cambridge University Press, New York, 1995), Chap. 3.